Supplementary Material (ESI) for Journal of Materials Chemistry

Supporting Information for

Facile tuning from blue to white emission in silica nanoparticles doped with oligothiophene fluorophores [§]

Manuela Melucci,[a,b]* *Massimo Zambianchi,*[a] *Giovanna Barbarella,*[a,c] *Ilse Manet,*[a] *Marco Montalti,*[d] *Sara Bonacchi,*[d] *Enrico Rampazzo,*[d] *Diana Cristina Rambaldi,*[d,e] *Andrea Zattoni,*[d,e] *Pierluigi Reschiglian*[d,e]

[a] Istituto per la Sintesi Organica e la Fotoreattività, (ISOF)-CNR, via Gobetti, 101, 40129 Bologna, Italy. Fax: (+39) (0)516398344; Tel: (+39) (0)516398271 and
[b] Istituto di Chimica dei Composti Organo Metallici-ICCOM-CNR, Via Madonna del Piano 10 50019 - Sesto Fiorentino- Florence – Italy, E-mail: mmelucci@isof.cnr.it
[c] Mediteknology Srl via Gobetti, 101, 40129 Bologna, Italy.
[d] Dipartimento di Chimica "G. Ciamician", Università degli Studi di Bologna, via Selmi, 2, 40126, Bologna, Italy
[e] I.N.B.B. Consortium, Rome, Italy

Contents:

1. AF4 separation mechanism

Separation is structured by the combined action of an axial, laminar flow and of a hydrodynamic field that is applied in perpendicular direction. The hydrodynamic field is generated because the flow entering the channel splits into two flow streams, one that goes to the longitudinal outlet (axial flow, Figure SI_1) and the other one that crosses the bottom

channel wall (cross-flow, Figure SI_1). Fractionation is structured by the combined action of the Brownian diffusion of the sample with the counteracting hydrodynamic field. The NPs of lower diffusion coefficient (green NPs; b, Figure SI_1) reach an equilibrium position that is closer to the channel wall than the position reached by NPs of higher diffusion coefficient (red NPs; a, Figure SI_1). This makes the different NPs be swept down the channel by streamlines at different velocities, which leads to NP separation: red NPs (a) elute earlier than green NPs (b). Retention times then result to be directly proportional to the hydrodynamic radius values of the different NPs.

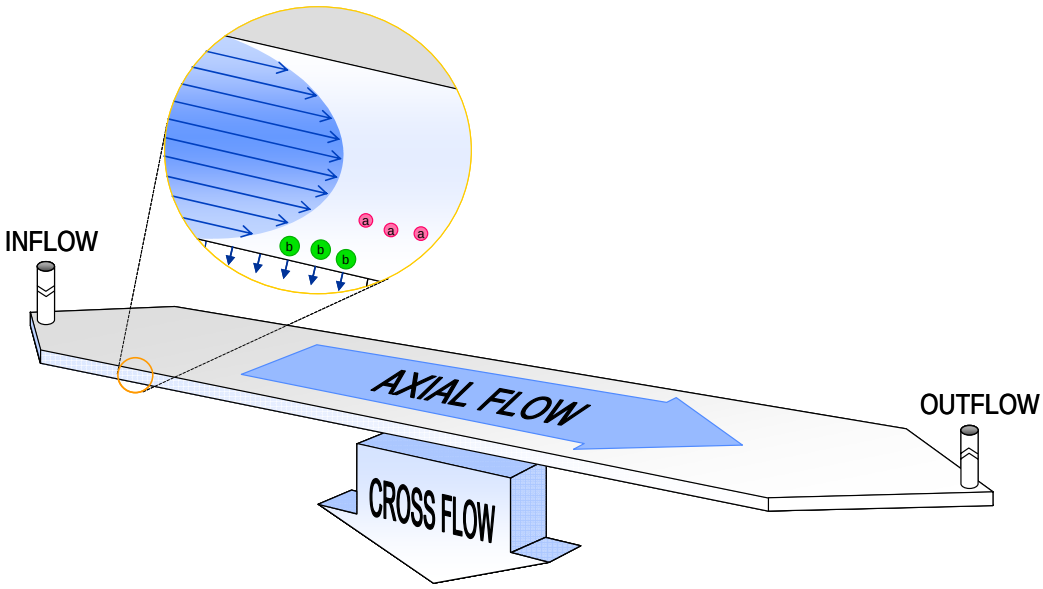

Figure SI_1.

2. AF4 channel layout

The AF4 channel is made of two machined blocks (walls) that clamp together a spacer and a membrane. The upper wall is in PEEK with an inset polycarbonate window for channel inspection. The bottom wall is also in PEEK with an inset stainless steel frit to generate the cross-flow stream. The bottom wall is covered up by an ultrafiltration membrane. The membrane selected in this study

is of regenerated cellulose with a pore cut-off of 10 kDa. The spacer is a PEEK sheet from which the channel geometry is cut out. The used AF4 channel dimensions are 24.0 x 2.15 x 0.0250 cm (length x width x thickness).

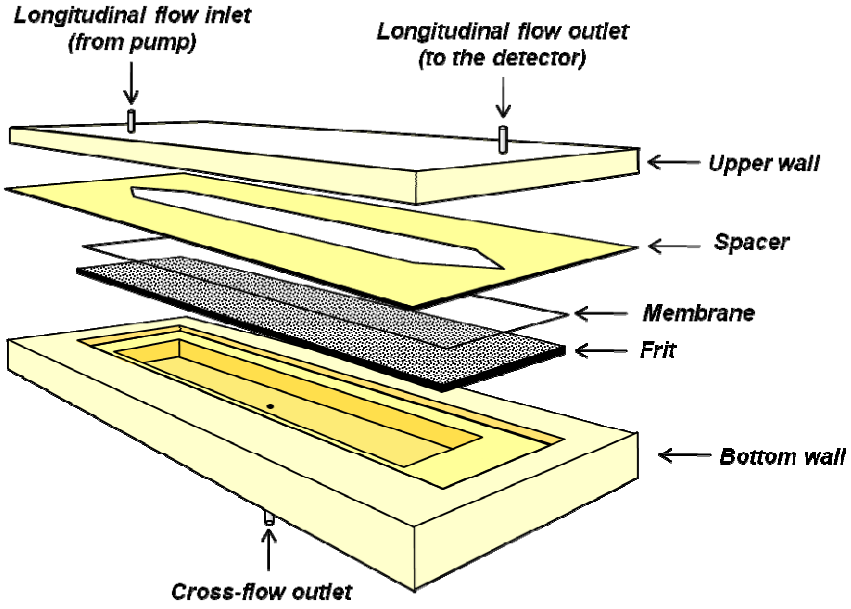

Figure SI_2

3. AF4-MALS-FD setup

The mobile phase is degassed, and delivered by an HPLC Pump. The sample is injected into the AF4 channel by means of an autosampler. The flow regimes are set and monitored by the AF4 Flow Controller. A multi-angle light scattering (MALS) detector and a fluorescence detector (FD) are connected downstream of the channel for detection and characterization of the eluted species.

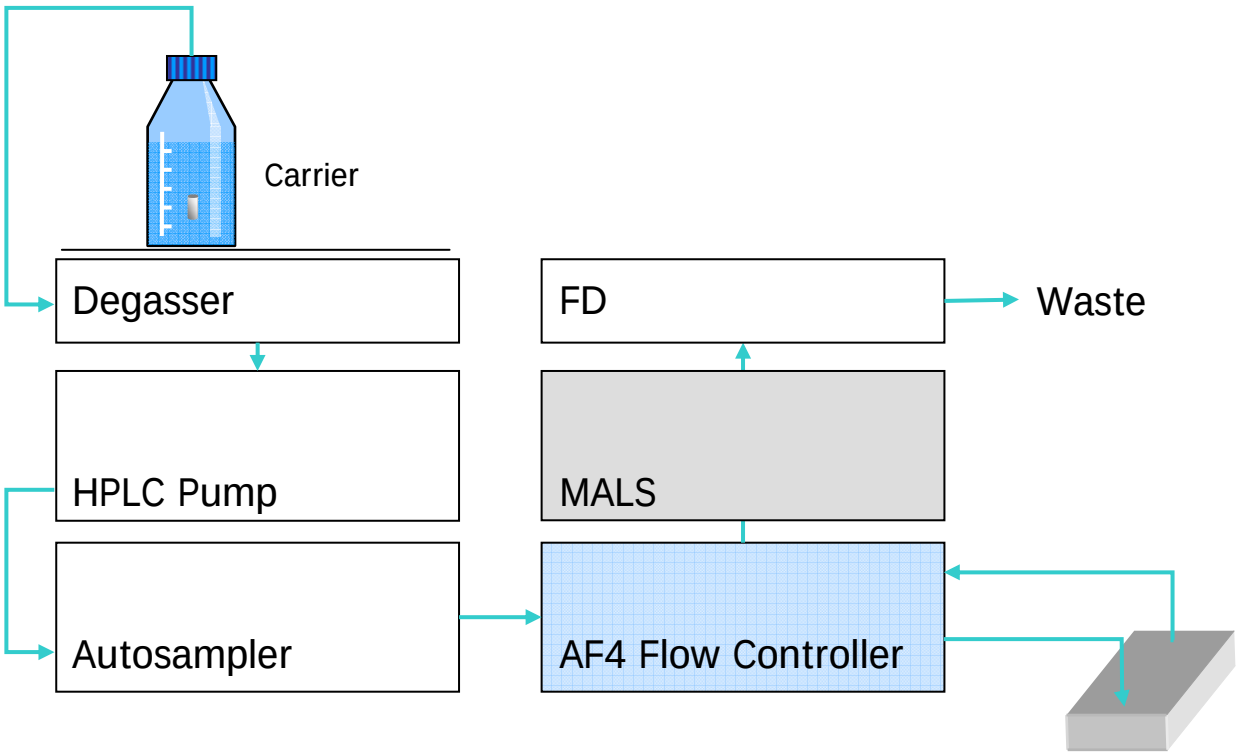

Figure SI_3.

4. Size distribution parameters calculated from MALS data

For each sample, data processing provided the following parameters: $\langle rms \rangle_n$ radius, z-averaged molar mass M_z, and number-averaged molar mass M_n values, which are defined according to the following expressions:

$$\langle \text{rms} \rangle_n \text{radius} = \frac{\sum_i r_{g_i} N_i}{\sum_i N_i} \quad \text{with} \quad \langle r_g \rangle^2 = \frac{\sum_j r_j^2 m_j}{\sum_j m_j}$$

$$M_z = \frac{\sum_i N_i M_i^3}{\sum_i N_i M_i^2}$$

$$M_n = \frac{\sum_i N_i M_i}{\sum_i N_i}$$

where r_i is the distance of the mass elements m_i from the particle center of mass; and N_j is the number of particles with molar mass M_j. In the ideal case of perfectly monodispersed particle populations, M_z and M_n coincide, while for real polydisperse samples, $M_z > M_n$. The polydispersity index M_z/M_n is thus equal to 1 for the ideal case of perfectly monodispersed samples, and it increases with increasing polydispersity.

$TfsSiO_2NPs$	$<rms>_n$ [nm]	M_z/M_n
B	38.0 ± 0.8	1.33 ± 2%
G	42.3 ± 0.8	1.35 ± 2 %
O	37.6 ± 0.8	1.32 ± 2 %
BG	49.0 ± 1.0	1.38 ± 3 %
BO	35.6 ± 0.7	1.37 ± 2%
GO	43.3 ± 0.9	1.38 ± 2 %
$BGO_{1:1:1}$	34.6 ± 0.7	1.14 ± 2%
$BGO_{3:1:1}$	39.7 ± 0.8	1.12 ± 2 %

Table 1. Number-averaged rms radius (<rms>n) and polidispersity (M_z/M_n) index values obtained by MALS for all the synthesized $TFsSiO_2NPs$.

5. Absorption and emission wavelengths, Stokes shift, and absorption band width for monocomponent $TFsSiO_2NPs$

Table SI_1. Summary of optical properties of B, G, O NPs in ethanol/H_2O 1:1.

NPs	**$\lambda_{max,abs}$ (nm)**	**$\lambda_{max,\ em.}$ (nm)**	**Stokes shift (nm/cm^{-1})[d]**	**Abs. band width [e] (nm)**
B	343	471[a]	128/7862	79
G	377	523[b]	146/7404	87
O	431	580[c]	149/5961	90

[a] λ_{exc}= 325 nm
[b] λ_{exc}= 400 nm
[c] λ_{exc}= 460 nm
[d] SS [cm^{-1}] = 10^7 / nm_{abs} – 10^7 / nm_{em}
[e] full width at the half-height

6. Energy transfer study

The energy transfer efficiency (η_{ET}) was calculated on the basis of quenching of the excitation energy donor: $\eta_{ET} = 1-(I/I_0)$, where I_0 and I are the fluorescence intensity of the donor in the absence and in the presence of the acceptor, respectively. [J. R. Lakowicz Principles of Fluorescence Spectroscopy, 3rd ed.; Springer: New York, 2006.].

Time-Correlated Single-Photon Counting (TCSPC) experiments were performed using an Edinburgh FLS920 equipped with photomultiplier Hamamatsu R928P and a PCS900 PC card.

A comparison with the spectra of mono-component $TFSiO_2NPs$ allowed calculating a FRET efficiency (ηET) as high as 90% for BG and BO, and 80% for GO NPs. The occurrence of energy transfer processes is confirmed by TCSPC measurements. The excited state lifetime of the blue emitting dye is, in fact, much shorter in the bi- and tri-component NPs ($\tau_B < 0.5$ ns) than in the mono-component NPs ($\tau_B = 2.9$ ns). On the other hand, in the presence of the energy acceptor O also the excited state lifetime of the green fluorophore decreases from $\tau_G = 1.1$ ns (in the mono-component NPs) to $\tau_G < 0.5$ ns.

7. Confocal Microscopy

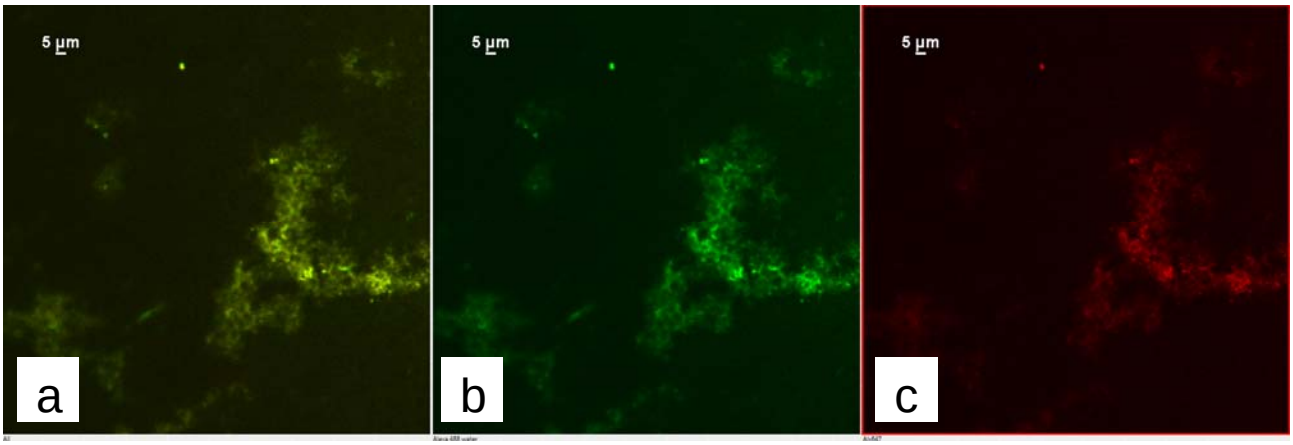

Figure SI_4. Confocal microscopy images showing dry clusters of BO NPs (λ_{exc}= 405 nm). a) image of the 500-550 nm emission channel (b) image of the 662-737 nm emission channel and (c) merged figure of the two channels overlap of images obtained by colour monitoring at 500-550.